tarjomehrooz.com 0902 795 28 76 ترجمه تخصصی توسط دکتری رشته مربوطه و برای کلیه زبان های خارجی + شبیه سازی مقالات با کلیه نرم افزار ها متلب گمز و ...

Energy Conversion and Management 79 (2014) 511–518

Contents lists available at ScienceDirect

Energy Conversion and Management

journal homepage: www.elsevier.com/locate/enconman

Evaluation of power flow solutions with fixed speed wind turbine generating systems

M.H. Haque *

School of Engineering, University of South Australia, Mawson Lakes 5095, Australia

ARTICLE INFO

Article history:
Received 5 April 2013
Accepted 23 December 2013
Available online 24 January 2014

Keywords:
Fixed speed wind generating system
Modeling of wind turbine generator
Power flow analysis
Renewable energy system
Squirrel-cage induction generator
Wind generator

ABSTRACT

An increased penetration of wind turbine generating systems into power grid calls for proper modeling of the systems and incorporating the model into various computational tools used in power system operation and planning studies. This paper proposes a simple method of incorporating the exact equivalent circuit of a fixed speed wind generator into conventional power flow program. The method simply adds two internal buses of the generator to include all parameters of the equivalent circuit. For a given wind speed, the active power injection into one of the internal buses is determined through wind turbine power curve supplied by the manufacturers. The internal buses of the model can be treated as a traditional *P–Q* bus and thus can easily be incorporated into any standard power flow program by simply augmenting the input data files and without modifying source codes of the program. The effectiveness of the proposed method is then evaluated on a simple system as well as on the IEEE 30- and 118-bus systems. The results of the simple system are also compared with those found through Matlab/Simulink using dynamic model of wind generating system given in SimPowerSystems blockset.

© 2014 Elsevier Ltd. All rights reserved.

1. Introduction

Wind is the fastest growing renewable energy technology in the world and is considered as the most cost effective way of generating electrical power from renewable sources. The principle of a wind turbine generating system (WTGS) is based on two well-known processes: conversion of kinetic energy of moving air into mechanical energy, and conversion of mechanical energy into electrical energy. The integration of WTGS into power grid has increased significantly in recent years [1]. In fact, worldwide installation of wind turbines has increased from about 5 GW in 1995 to more than 275 GW in 2012 [2]. Increased penetration of wind generators into power grid calls for proper modeling of the WTGS and incorporating the model into various computational tools used for steady state and dynamic analyses of power systems.

A WTGS can be classified into fixed speed, limited variable speed and variable speed [3,4]. The fixed speed (or Type-1) generating system employs a squirrel-cage induction generator (SCIG) which is directly connected to the grid through a step-up transformer. A soft starter and shunt capacitors are usually used for smoother connection and reactive power support. A SCIG operates within a very narrow speed range (around the synchronous speed) and that is why it is considered as a fixed speed generator. The limited variable speed (or Type-2) generating system employs a wound-rotor induction generator (WRIG). The speed of the generator can be varied within a certain range by adjusting external rotor impedance of the generator. The variable speed generating system requires either partial-size or full-size converters. The generating system with partial-size converters (or Type-3) employs a doubly feed induction generator (DFIG). The rotor excitation of the DFIG is supplied by a current regulated voltage source converter, which adjusts the magnitude and phase angle of rotor current almost instantly. The rotor side converter is connected back-to-back to a grid side converter. The generating system with full-size converter (or Type-4) usually employs a permanent magnet synchronous generator (PMSG), which is connected to the grid through full size back-to-back voltage source converters or a diode rectifier and a voltage source converter.

In terms of power control, a wind turbine (WT) can be classified into stall-controlled and pitch-controlled [5,6]. A stall-controlled WT has a fixed blade angle but the blades are carefully designed to reduce aerodynamic efficiency at higher wind speeds to prevent the extraction of excessive power from the wind. On the other hand, a pitch-controlled WT adjusts the blade pitch angle to limit the power capture at higher wind speeds. Most of the earlier wind farms used fixed speed stall-controlled wind turbines [7]. A fixed speed WT is also known as "Danish concept" as it was developed and widely used in Danish wind farms. However, the present trend is to use variable speed WTs that employ DFIGs. In both cases, it is very important to incorporate the model of WTGS into existing computational tools used in power system studies.

* Tel.: +61 8 8302 3285; fax: +61 8 8302 3384.
E-mail address: mohammed.haque@unisa.edu.au

0196-8904/$ - see front matter © 2014 Elsevier Ltd. All rights reserved.
http://dx.doi.org/10.1016/j.enconman.2013.12.049

tarjomehrooz.com 0902 795 28 76 ترجمه تخصصی توسط دکتری رشته مربوطه و برای کلیه زبان های خارجی + شبیه سازی مقالات با کلیه نرم افزار ها مثلب گمز و ...

The steady state behavior of a power system is usually evaluated through power flow calculations which mainly determine the complex voltage (magnitude and phase angle) of all buses. The complex power flow through each branch and other quantities are then calculated using the complex bus voltages. In power flow calculations, the buses of a power system are classified into swing (or V-δ) bus, voltage-controlled (or P-V) bus and load (or P–Q) bus [8,9]. For a P–V or a P–Q bus, the active power injection P into the bus is known or specified. Fortunately, most of the WT manufacturers provide the power curve (mechanical power verses wind speed) of the turbine [10,11]. By knowing wind speed, the corresponding turbine mechanical power can immediately be determined from the curve.

In power flow analysis, a fixed speed wind generating system is usually represented by a P–Q model or an R-X model [12–16]. In P–Q model, the reactive power drawn by the generator is first approximated in terms of its active power and terminal voltage. The per-phase steady state equivalent circuit of the generator, with some approximations, is used for this purpose. For a given wind speed, the generator bus is treated as a P–Q bus with varying reactive power, in contrast to a conventional P–Q bus where it remains constant. This model may not provide correct results because of the approximations used in evaluating the reactive power. An accurate P–Q model of a SCIG is described in [16] but the model need to be evaluated as a part of the iterative process of the power flow program. A DFIG or a PMSG can also be represented by a P–Q model with varying reactive power as it is controlled by the converter. Such generators can also be operated either as constant power factor mode or constant voltage mode.

In R-X model, a SCIG generator is represented by an equivalent impedance obtained from its steady state equivalent circuit [12,13]. In power flow analysis, the impedance is then considered as a shunt element at the generator terminal bus. However, the impedance of the generator is not constant but highly dependent on operating slip which is not known *apriori*. In [12], a sub-problem is formulated to calculate the slip iteratively. Alternatively, the jacobian of the power flow program can be modified to include the slip [17]. In both cases, significant modifications to the source codes of the program are needed.

This paper proposes a simple method of incorporating the exact equivalent circuit of a fixed speed wind generator into a power flow program that does not require any modification to source codes of the program. The method simply augments the network by two internal buses of the generator to include all parameters of the exact equivalent circuit of the generator. The proposed method is then tested on a simple system as well as on the IEEE 30- and 118-bus systems.

2. Power flow method

Power flow is one of the most important computational tools used in power system operation and planning studies. It solves the active and reactive power equations to find bus voltage magnitudes and phase angles. The injected active power (P_i) and reactive power (Q_i) into bus i of an n-bus power system can be written as [8]

$$P_i = V_i^2 G_{ii} + V_i \sum_{j=1;\neq i}^{n} V_j (B_{ij} \sin\delta_{ij} + G_{ij} \cos\delta_{ij}) \quad (1)$$

$$Q_i = -V_i^2 B_{ii} + V_i \sum_{j=1;\neq i}^{n} V_j (G_{ij} \sin\delta_{ij} - B_{ij} \cos\delta_{ij}) \quad (2)$$

Here $\mathbf{Y} = (G + jB)$ and $\delta_{ij} = (\delta_i - \delta_j)$. V_i and V_j are the voltage magnitude of buses i and j, respectively. δ_i and δ_j are the voltage phase angle of buses i and j, respectively, and $\mathbf{Y}$ is the bus admittance matrix.

The Newton Raphson (NR) method is commonly used to solve the above equations. The governing equation of the method can be written as

$$\begin{bmatrix} \Delta P \\ \Delta Q \end{bmatrix} = \begin{bmatrix} \frac{\partial P}{\partial \delta} & \frac{\partial P}{\partial V} \\ \frac{\partial Q}{\partial \delta} & \frac{\partial Q}{\partial V} \end{bmatrix} \begin{bmatrix} \Delta \delta \\ \Delta V \end{bmatrix} \equiv [J] \begin{bmatrix} \Delta \delta \\ \Delta V \end{bmatrix} \quad (3)$$

The size of the jacobian matrix J in (3) is $(n_{PV} + 2n_{PQ}) \times (n_{PV} + 2n_{PQ})$, where n_{PV} is the number of P-V buses and n_{PQ} is the number of P–Q buses in the system. The computational algorithm of the method is well described in literature [8,9]. For most of the well-behaved systems, the NR method usually converges in 3–6 iterations.

3. Wind power

The mechanical power captured by a wind turbine (P_T) can be written as [18,19]

$$P_T = \frac{1}{2} \rho A V_w^3 C_p(\lambda, \beta) \quad (4)$$

Here ρ is the air density (kg/m^3), A is the turbine blade swept area (m^2), V_w is the wind speed (m/s), and C_p is the performance coefficient of the turbine. C_p is a function of tip speed ratio λ and blade pitch angle β, and it can be expressed as [19]

$$C_p(\lambda, \beta) = c_1 \left[\frac{c_2}{\lambda_i} - c_3\beta - c_4\beta^{c_5} - c_6 \right] \exp\left(\frac{-c_7}{\lambda_i} \right) \quad (5)$$

where $\lambda_i = \left[\frac{1}{\lambda + c_8\beta} - \frac{c_9}{\beta^3 + 1} \right]^{-1}$ and $\lambda = \frac{R\omega_T}{V_w} = \frac{R a_g \omega_r}{V_w}$

Here ω_T and ω_r are the angular velocity (rad/s) of the turbine and the generator rotor, respectively. R is the turbine blade length (m) and a_g is the gear ratio. The value of various constants (c_1–c_9) can be determined from manufacturer data. The above equations are very useful in designing control system of a WT to maximize its efficiency. However, the objective of this paper is to determine the power flow results of a wind integrated power system and the evaluation of control strategy of WT is beyond the scope of the paper.

A typical variation of turbine power against wind speed is shown in Fig. 1 where V_{in}, V_r and V_{out} represent the cut-in wind speed, rated wind speed and cut-out wind speed, respectively,

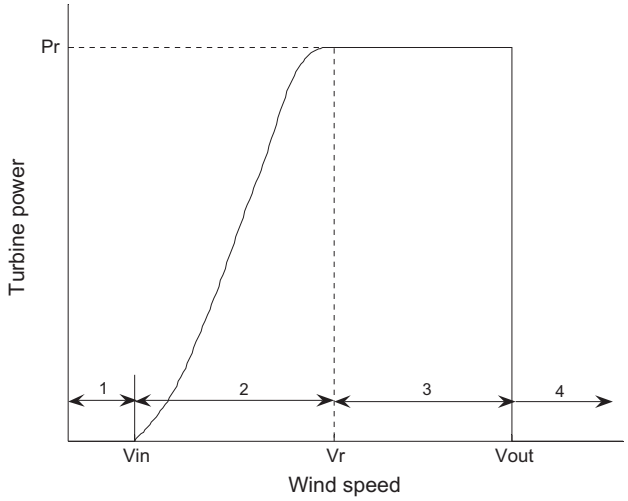

Fig. 1. Typical power curve of a wind turbine.

tarjomehrooz.com 0902 795 28 76 ترجمه تخصصی توسط دکتری رشته مربوطه و برای کلیه زبان های خارجی + شبیه سازی مقالات با کلیه نرم افزار ها مثلب گمز و ...

and P_r is the rated power of the turbine. It can be noticed in Fig. 1 that the turbine power is variable only in region 2 where the wind speed varies between V_{in} and V_r. In other regions (1, 3 and 4) or wind speeds, the turbine power is either zero or at rated value. Fortunately, most of the WT manufacturers provide the power curve and thus for a given wind speed, the turbine power can immediately be determined from the curve or a lookup table. In simulation studies, it is preferable to have piece-wise mathematical expressions of the power curve. Refs. [20,21] estimated the power in region 2 ($V_{in} \leqslant V_w \leqslant V_r$) through a quadratic function using the values of V_{in}, V_r and P_r. In this study, the turbine power P_T in region 2 is expressed by the following polynomial

$$P_T = a_0 + a_1 V_w + a_2 V_w^2 + a_3 V_w^3 \tag{6}$$

The manufacturer data can be used to evaluate the coefficients a's of (6) using any standard curve fitting technique. Fig. 2 shows a comparison of estimated power obtained through (6) with the corresponding actual values of Vestas V100-1.8 MW wind turbine supplied by the manufacturer [10]. The coefficients of (6) are obtained through 'polyfit' routine given in MATLAB using the manufacturer data extracted at discrete wind speeds (at an interval of 1 m/s) from cut-in wind speed of 3 m/s to rated wind speed of 12 m/s.

Thus, mathematically, the turbine power P_T of Fig. 1 can be expressed as

$$P_T = \begin{cases} 0; & \text{if } V_w \leqslant V_{in} \\ (a_0 + a_1 V_w + a_2 V_w^2 + a_3 V_w^3); & \text{if } V_{in} \leqslant V_w \leqslant V_r \\ P_r; & \text{if } V_r \leqslant V_w \leqslant V_{out} \\ 0; & \text{if } V_w > V_{out} \end{cases} \tag{7}$$

A small fraction of turbine power is lost in the gearbox and the remaining power can be considered as input mechanical power P_m to the generator. Thus,

$$P_m = \eta_g P_T \tag{8}$$

Here η_g is the efficiency of the gear box. The generator converts mechanical power P_m into electrical power and feeds into the grid. The objective of this study is to properly model the WTGS and incorporate the model into a conventional power flow program to evaluate the steady state results of the system.

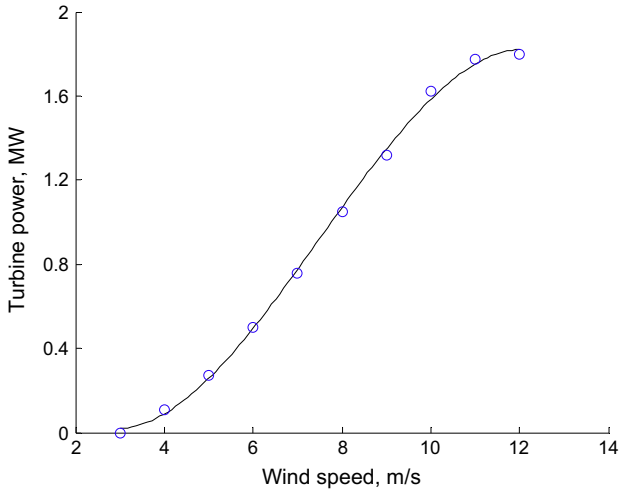

Fig. 2. Comparison of estimated and actual turbine power, '—' estimated through (6); '○' manufacturer supplied data.

4. Model of WTGS and its incorporation into power flow program

Consider that the SCIG of a fixed speed WTGS is connected to bus k of a general power system through a step-up transformer as shown in Fig. 3. An external shunt capacitor is also connected to the generator terminal to supply reactive power. Note that a SCIG always absorbs reactive power and that can be compensated by the external shunt capacitor. Alternatively, a static var compensator (SVC) or a static synchronous compensator (STATCOM) can be used to support reactive power. By selecting appropriate size of shunt capacitors and/or SVC/STATCOM, the terminal voltage of the generator can be regulated.

The equivalent circuit of the SCIG including the transformer and the shunt capacitor is shown in Fig. 4 where R_1, R_2, X_1, X_2 and X_m represent the stator resistance, rotor resistance, stator leakage reactance, rotor leakage reactance and magnetizing reactance, respectively, of the generator, and s is the slip. $R_t + jX_t$ and $-jX_c$ represent the impedance of the transformer and the shunt capacitor, respectively.

The power of the rightmost resistance $R_2(1-s)/s$ of Fig. 4 represents the input mechanical power P_m to the generator and is supplied by the WT. Note that, for generator operation, slip s is negative and thus the power absorbed by the resistance is also negative. By knowing wind speed V_w, P_m can be determined through (7) and (8). The generator converts P_m into electrical power and delivers a complex output power ($P_e + jQ_e$) at its terminal (see Fig. 4). The difference between P_m and P_e represents the losses in R_1 and R_2. Note that the generator draws reactive power from the system and thus Q_e is negative. In fact, $-Q_e$ is the sum of reactive power losses in X_1, X_m and X_2.

The circuit of Fig. 4 is redrawn in Fig. 5 by explicitly showing two internal buses (m and r) of the generator in addition to the terminal bus t and the system bus k. Bus m represents the air–gap line where the magnetizing reactance X_m is connected and bus r represents a fictitious rotor internal bus where the WT supplies mechanical power P_m to the generator. In Fig. 5, the power supplied by the WT is represented as negated load of $-P_m + j0$. Most of the previous methods [12–16] considered only the generator terminal bus t and determined the complex power ($P_e + jQ_e$) with some approximations or through significant modifications of computational algorithm of the power flow program. However, the proposed method extends the generator model beyond the terminal bus to include all parameters of the exact equivalent circuit of the generator. It may be mentioned here that the core loss resistance of the generator can also be included in parallel with jX_m at bus m.

By looking into Fig. 5, one can easily recognize that it is simply a radial system consisting of four buses (k, t, m and r), three series elements ($R_t + jX_t$, $R_1 + jX_1$ and $R_2 + jX_2$), two shunt elements ($-jX_c$ and jX_m) and a load ($-P_m + j0$) at bus r. The usual values of generator parameters ($R_1 \ll X_1$, $R_2 \ll X_2$, and higher value of X_m) and load at bus r would allow to find the power flow solutions of the system using any standard power flow program by carefully incorporating the parameters of Fig. 5 into input data files (bus data and line

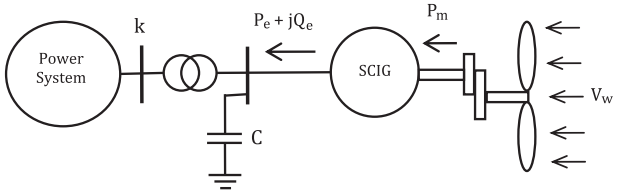

Fig. 3. Schematic diagram of a fixed speed WTGS connected to a power system through a transformer.

tarjomehrooz.com 0902 795 28 76 ترجمه تخصصی توسط دکتری رشته مربوطه و برای کلیه زبان های خارجی + شبیه سازی مقالات با کلیه نرم افزار ها مثلب گمز و ...

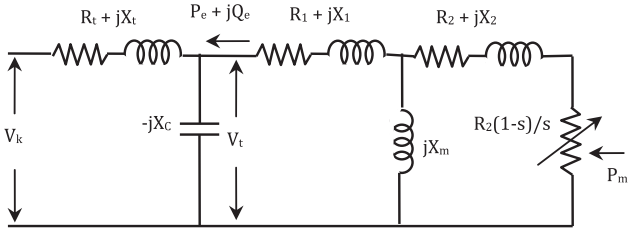

Fig. 4. Equivalent circuit of a fixed speed WTGS including the transformer and shunt capacitor.

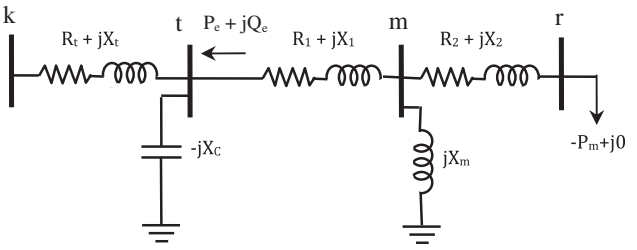

Fig. 5. Single-line representation of Fig. 4.

data) without modifying source codes of the program. Note that a similar model is also used in [22,23] to represent an induction motor load in determining system loadability through power flow calculations.

As mentioned, a power flow program mainly determines the voltage magnitude and phase angle of all buses which are then used to compute power flow of all branches and other quantities. The complex power flow through branch $R_1 + jX_1$ near bus t (as shown in Fig. 5) represents the complex power ($P_e + jQ_e$) supplied by the generator at its terminal. The results associated with the internal buses (m and r) of Fig. 5 are not important and thus may be ignored or suppressed in the output of the program.

5. Results and discussions

The model of a fixed speed WTGS and its incorporation into a conventional power flow program is vigorously tested on the following three systems:

1. A simple infinite bus system.
2. The IEEE 30-bus system.
3. The IEEE 118-bus system.

In the IEEE 30- and 118-bus systems, a number of wind farms (WF) are added throughout the network. It is considered that each wind farm consists of a number of identical Vestas wind turbine (V100-1.8-MW) and SCIG (1.8-MW, 575-V, 0.9-pf) sets. A brief description of wind farms used in this study is given in Table 1. The power curve of the WT is obtained from [10] and it has a cut-in, rated and cut-out wind speed of 3, 12 and 25 m/s, respectively.

Table 1
Summary of various wind farms used in the IEEE 30- and 118-bus systems.

Wind farm	Number of WT and SCIG sets	Capacity in MW/MVA
A	5	9/10
B	10	18/20
C	15	27/30
D	20	36/40
E	25	45/50
F	30	54/60

Even though the curve is for a pitch-controlled variable speed turbine but the same data is used in this study because of the lack of actual data for a large size fixed speed turbine. Ref. [24] demonstrated that the power curve of a pitch-controlled fixed speed WT is not significantly different than that of a variable speed WT. The gear efficiency η_g of the turbine is arbitrarily assumed as 95%. The parameters of the generator are considered as $R_1 = 0.004843$ pu, $X_1 = 0.1248$ pu, $R_2 = 0.004377$ pu, $X_2 = 0.1791$ pu, and $X_m = 6.77$ pu. The leakage reactance of the step-up transformer is assumed as 0.05 pu.

The power flow results of the above three systems are obtained by the NR method. The NR power flow program given in Power Toolbox [9] as well as developed in [25] is used for this purpose and both programs provide the same results. The results obtained in the above three systems are briefly described in the following.

5.1. A Simple infinite bus system

Consider that a fixed speed WTGS is connected to an infinite bus through a step-up transformer and a short transmission line. Such a system can be represented by Fig. 5 when the line impedance and the transformer impedance are combined. The data of the system is given in the Appendix. The system is also implemented in Matlab/Simulink using dynamic model of the turbine-SCIG set given in SimPowerSystems blockset [26]. The Matlab/Simulink block diagram of the system is shown in Fig. 6. It may be mentioned here that the steady state values of dynamic response of Fig. 6 should represent the power flow results. In Fig. 6, the wind speed is increased from 6.5 m/s to 9 m/s in step of 0.5 m/s and the corresponding dynamic response of the system (including wind speed) is shown in Fig. 7 which indicates that the active power increases as the wind speed is increased. At a higher wind speed, the generator draws more reactive power because of higher losses in X_1 and X_2 due to higher currents. It is interesting to notice that the terminal voltage initially increases with the increase in wind speed and then starts decreasing at higher wind speeds. It is worth mentioning that, for a given system voltage at bus k (in Fig. 5), delivery of active power P_e increases the voltage at bus t but drawing of reactive power Q_e reduces the voltage at bus t. The ultimate voltage at bus t depends on the values of P_e and Q_e as well as the R/X ratio of the transformer and line impedances.

The power flow results of the system of Fig. 5 are also obtained by the NR method for various wind speeds or mechanical power P_m (as used in Fig. 6). Table 2 shows a comparison of results obtained by the NR method and the corresponding steady state values found through Matlab/Simulink dynamic simulations and it indicates that the results are in excellent agreement. The maximum error observed is only 0.56%. Using the power flow results, the slips and hence speeds of the generator are also determined by equating $-P_m$ with $V_r^2/[R_2(1-s)/s]$ and are found to be exactly the same as the steady state values of generator speed shown in Fig. 7.

5.2. The IEEE 30-bus system

The single line diagram and data of the IEEE 30-bus system are given in [9]. The system is modified by adding three wind farms A, B and C (as described in Table 1) at buses 14, 26 and 30, respectively. The network of the system is then augmented to include the model of the wind farms. In the augmented network, the generator terminal bus (bus t in Fig. 5) of wind farms A, B and C is numbered as 31, 34 and 37, respectively. The wind speed of wind farms A, B and C is arbitrarily assumed as 12, 10 and 8 m/s, respectively.

The power flow of the augmented network is then evaluated without and with shunt capacitors. The MVAr rating of shunt capacitors is considered as 25% of respective wind farm capacity in MVA. The power flow of the system is also evaluated at higher

tarjomehrooz.com 0902 795 28 76 ترجمه تخصصی توسط دکتری رشته مربوطه و برای کلیه زبان های خارجی + شبیه سازی مقالات با کلیه نرم افزار ها مثلب گمز و ...

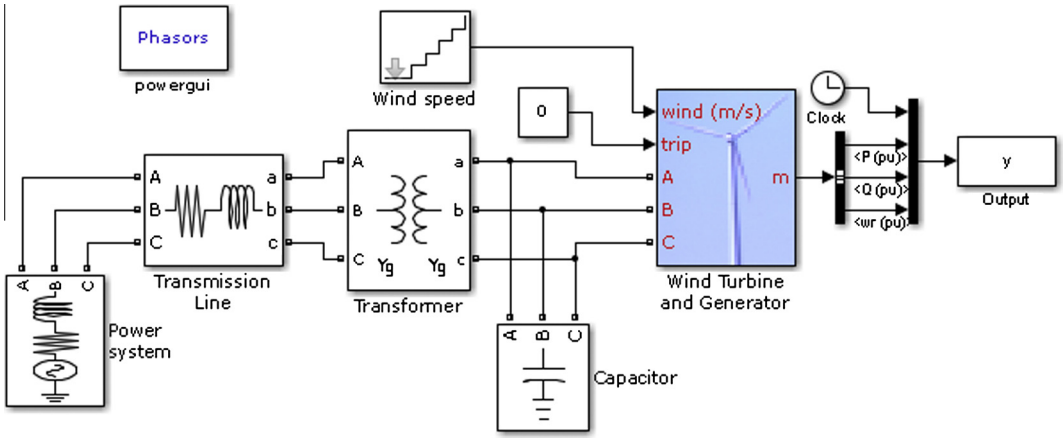

Fig. 6. Matlab/Simulink block diagram of the simple system.

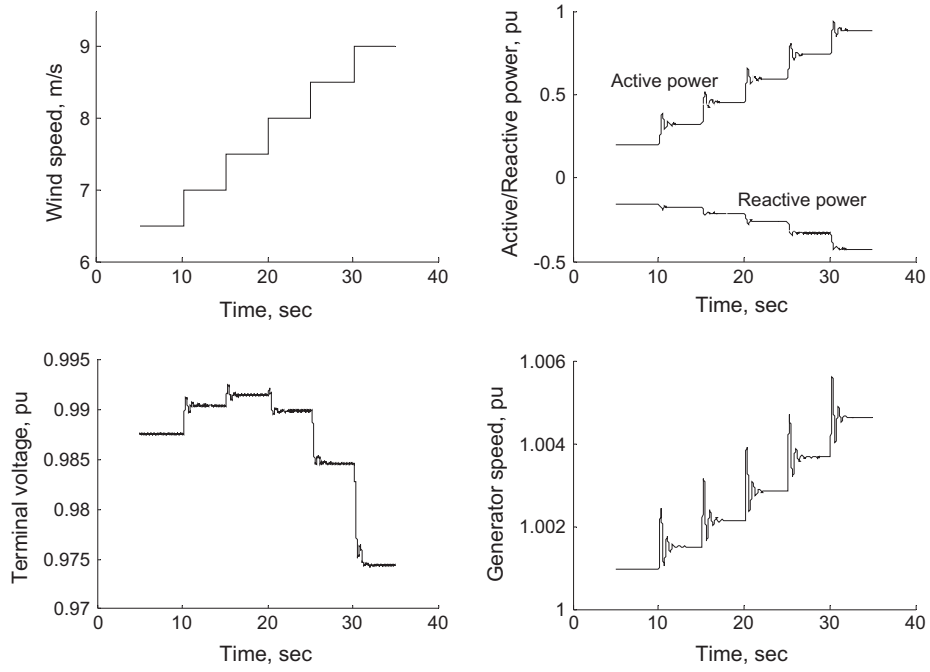

Fig. 7. Dynamic responses of the simple system.

Table 2
Comparison of results of the simple system obtained through Newton Raphson (NR) method and SimPowerSystems (SPS) blockset.

V_w (m/s)	P_m (pu)	Voltage V_t (pu)		Complex power $P_e + jQ_e$ (pu)	
		NR	SPS	NR	SPS
6.5	0.2034	0.9877	0.9876	0.2029 – j0.1550	0.2026 – j0.1553
7.0	0.3247	0.9906	0.9905	0.3235 – j0.1765	0.3229 – j0.1769
7.5	0.4582	0.9916	0.9915	0.4560 – j0.2109	0.4547 – j0.2113
8.0	0.6007	0.9900	0.9899	0.5969 – j0.2613	0.5947 – j0.2614
8.5	0.7489	0.9847	0.9847	0.7428 – j0.3315	0.7395 – j0.3310
9.0	0.8999	0.9742	0.9744	0.8907 – j0.4284	0.8857 – j0.4264

wind speeds ($V_r < V_w < V_{out}$) to operate the wind farms at their rated capacity. In all cases, the NR method successfully converged in 4–5 iterations. Table 3 shows a comparison of voltage at system buses 14, 26 and 30 as well as generator terminal buses 31, 34 and 37. The voltage of buses 14, 26 and 30 in the original system (without wind farms) is also shown in the Table for comparison purpose. It can be noticed in Table 3that the wind farms (without having shunt capacitors) slightly reduce the bus voltage because of drawing reactive power. However, the voltage profile is improved when the shunt capacitors are added. At higher wind speeds (with shunt capacitors), the voltage profile again decreases because of drawing more reactive power.

5.3. The IEEE 118-bus systems

The single line diagram of the IEEE 118-bus system is given in [27] and it has a base load of (3848.0 + j952.0) MVA. The system is modified by adding 12 wind farms throughout the network. Table 4 shows the buses at which the wind farms are added including the wind speeds and the generator terminal buses in the augmented network. The power flow of the system is then evaluated for the following five cases:

1. Original system (without wind farms).
2. Modified system without shunt capacitor.

tarjomehrooz.com 0902 795 28 76 ترجمه تخصصی توسط دکتری رشته مربوطه و برای کلیه زبان های خارجی + شبیه سازی مقالات با کلیه نرم افزار ها مثلب گمز و ...

Table 3
Comparison of voltage at some buses of the IEEE 30-bus system.

Bus no.	Original system	Modified system with 3 wind farms		
		Without capacitor	With capacitor	At higher wind speeds
14	1.042	1.038	1.049	1.046
26	1.001	0.986	1.051	1.034
30	0.995	0.971	1.042	1.016
31	–	1.018	1.043	1.040
34	–	0.968	1.047	1.027
37	–	0.959	1.044	1.013

Table 4
Description of wind farms used in the IEEE 30-bus system.

Network bus (k)	Wind farm	Wind speed (m/s)	Generator terminal bus (t)
3	A	16	119
16	B	14	122
20	C	12	125
33	D	10	128
41	E	8	131
53	F	6	134
62	A	12	137
74	B	11	140
84	C	10	143
98	D	9	146
106	E	8	149
117	F	7	152

3. Modified system with shunt capacitor.
4. Modified system at higher wind speeds without shunt capacitor.
5. Modified system at higher wind speeds with shunt capacitor.

In last two cases, the wind speed of all wind farms is increased to 15 m/s to operate the farms at rated capacity. The MVAr rating of shunt capacitors is again considered as 25% of respective wind farm capacity in MVA. In all cases, the NR method successfully converged in 5 iterations.

Fig. 8 shows a comparison of voltage of some buses of the original network (bus *k* in Fig. 5) for all five cases (in sequence) and it indicates that the voltage profile depends on both the wind speeds and the shunt capacitors but the variation in voltage is not significant. For bus 62, it is found that the voltage remains more of less constant for all cases because the bus is very strong (with a load of 77 MW) and a small wind farm (only 9 MW) is connected to it. The maximum voltage deviation is observed as 0.039 pu and that occurred at bus 117 (between cases 3 and 4). A comparison of generator terminal voltage in the augmented network for the last four cases (in sequence) is also shown in Fig. 9 and it again indicates that the voltage depends on both wind speeds and shunt capacitors but the voltage variation is again not significant. The maximum deviation is observed as 0.065 pu at bus 152.

The power flow of the system is also evaluated at low wind power by setting the wind speed of all farms to a lower value. For a wind speed of 4.5 m/s, the total wind power is found as 32.35 MW (8.6% of installed capacity) and for such a case the minimum system voltage with and without shunt capacitors is found as 0.9519 pu and 0.9359 pu, respectively. In both cases, the maximum voltage is found as 1.05 pu (which is the specified voltage at one of the conventional generator buses). Since the penetration level of wind power is not high (installed capacity is less than 10% of system demand), lower or even zero wind power may not change the voltage profile significantly, especially for a strong system.

Finally, the wind speed of all wind farms is randomly selected through Weibull probability density function with a shape parameter of 2 and scale parameter of 9.027 (that corresponds to an average wind speed of 8 m/s [28]) using 'random' routine given in Matlab. The power flow problem of the modified network with shunt capacitors is then repeatedly solved for 1000 random cases of wind speeds. In all cases, the NR method successfully converged within 5 iterations. The distribution of total injected wind power (at internal bus *r*) is shown in Fig. 10(a). The minimum and the maximum power for 1000 random cases are found as 47.19 MW and 333.94 MW, respectively. Note that the total capacity of 12 wind farms is 378 MW. The distribution of minimum bus voltage of the original network (buses 1–118) is shown in Fig. 10(b) and it indicates that the minimum voltage varies within a very narrow range (0.9419 pu – 0.9543 pu) possibly because of low degree of penetration of wind power (<10%). However, the minimum voltage in the augmented network including the generator terminal and internal buses has a wider range (0.8712 pu – 0.9400 pu) as can be seen in Fig. 10(c). In all

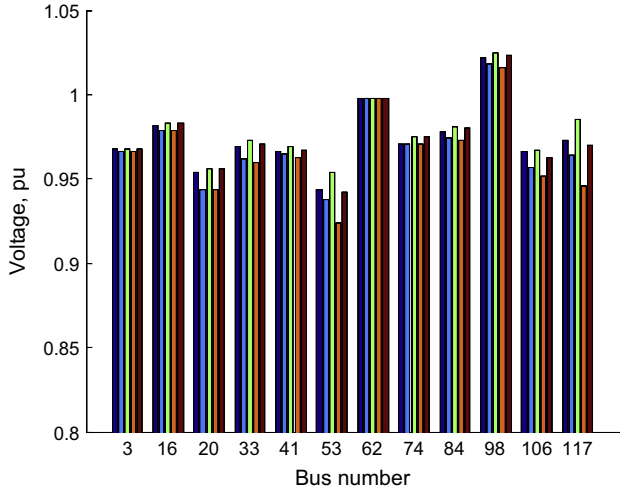

Fig. 8. Voltage profile of some buses of the IEEE 118-bus system.

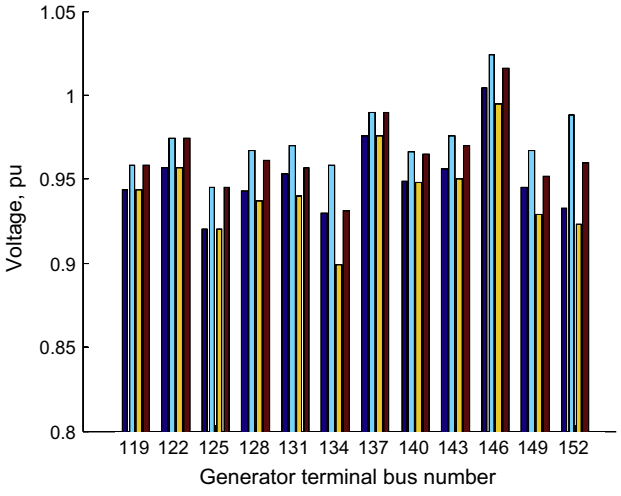

Fig. 9. Voltage profile of wind generator terminal buses of the IEEE 118-bus system.

tarjomehrooz.com 0902 795 28 76 ترجمه تخصصی توسط دکتری رشته مربوطه و برای کلیه زبان های خارجی + شبیه سازی مقالات با کلیه نرم افزار ها مثلب گمز و ...

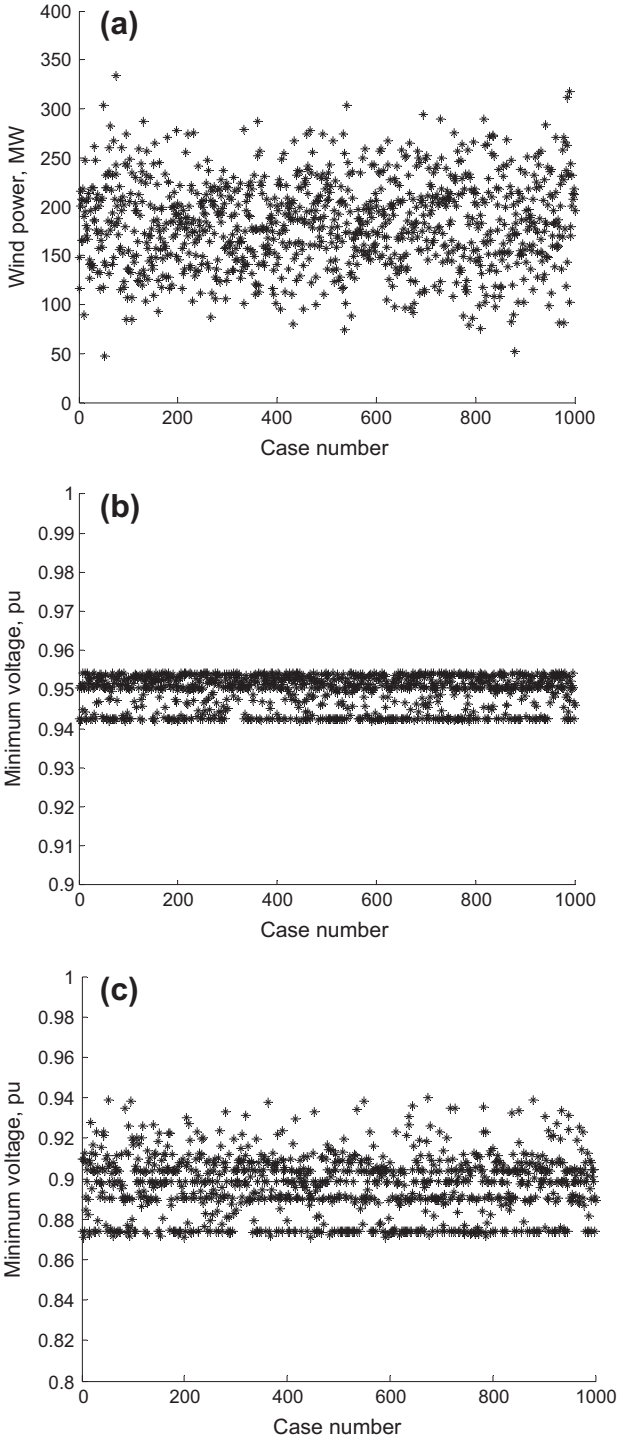

Fig. 10. Distribution of results of the 118-bus system for 1000 random cases of wind speeds: (a) wind power, (b) minimum voltage of buses 1–118, (c) minimum voltage in the augmented network.

cases, the lowest voltage occurred at generator internal buses and which is not so important.

6. Conclusions

A simple method of incorporating the exact equivalent circuit of a fixed speed wind generating system into a conventional power flow program has been presented in this paper. The method simply augmented the network by adding two internal buses for each generating system. The new buses have the same property as a *P*–*Q* bus and thus can easily be incorporated into any power flow program without modifying the source codes of the program. However, augmentation of input data files of the program is needed to include the model or parameters of the generating system. The effectiveness of the proposed method is then vigorously tested on a simple system as well as on the modified IEEE 30- and 118-bus systems. The power flow results of the simple system were also compared with the corresponding steady state values of dynamic responses of the system and are found to be in excellent agreement. It is also found that the incorporation of wind generators does not affect the convergence pattern of the power flow program.

Appendix A

Data of the Simple Infinite Bus System:

Generator:	1.5-MW, 575-V, 60-Hz, 6-pole, 0.9-power factor R_1 = 0.004843 pu, X_1 = 0.1248 pu, R_2 = 0.004377 pu, X_2 = 0.1791 pu, X_m = 6.77 pu, H = 5.04 s
Transformer:	2 MVA, 11 kV/575 V, R = 0.02 pu, X = 0.08 pu
Transmission line:	11 kV, R = 3 Ω, X = 6 Ω
Infinite bus:	11 kV with infinite short circuit level.

References

[1] Smith JC, Parsons B. Wind integration – much has changed in two years. IEEE Power Energy Mag 2011;9(6):18–25.
[2] <http://www.thewindpower.net/index.php>.
[3] Li H, Chen Z. Overview of different wind generator systems and their comparisons. IET Renew Power Gener 2008;2(2):123–38.
[4] IEEE PES Wind Plant Collector System Design Working Group. Characteristics of wind turbine generators for wind power plants. In: Proc. 2009 IEEE power and energy society general meeting, Calgary, Canada, July 2009.
[5] Muljadi E, Butterfield CP. Pitch-controlled variable-speed wind turbine generation. NREL, Report No. NREL/CP-500-27143, 2000.
[6] Slootweg JG, Polinder H, Kling WL. Representing wind turbine electrical generating systems in fundamental frequency simulations. IEEE Trans Energy Conversion 2003;18(4):516–24.
[7] Hansen AD, Hansen LH. Wind turbine concept market penetration over 10 years (1995–2005). Wind Energy 2007;10:81–97.
[8] Kundur P. Power system stability and control. McGraw-Hill; 1993.
[9] Saddat H. Power system analysis. McGraw-Hill; 1999.
[10] <http://www.vestas.com/en/media/brochures.aspx>.
[11] <http://www.energy.siemens.com/mx/en/power-generation/renewables/wind-power/wind-turbines/>.
[12] Feijoo AE, Cidras J. Modeling of wind farms in the load flow analysis. IEEE Trans Power Syst 2000;15(1):110–5.
[13] Eminoglu U. Modelling and application of wind turbine generating systems (WTGS) to distribution systems. Renew Energy 2009;34:2474–83.
[14] Divya KC, Rao PSN. Models for wind turbine generating systems and their application in load flow studies. Electric Power Syst Res 2006;76:844–56.
[15] Liu Y, Wang W, Xu L, Ni P, Wang L. Research on power flow algorithm for power system including wind farm. Proc Int Conf Electric Mach Syst 2008:2551–5.
[16] Feijoo A. On PQ models for asynchronous wind turbines. IEEE Trans Power Syst 2009;24(4):1890–1.
[17] Esquivel CRF, Hermandez JHT, Alcaraz GG, Torres FC. Discussion of modelling of wind farms in the load flow analysis. IEEE Trans Power Syst 2001;16(4):951.
[18] Heier S. Grid integration of wind energy conversion systems. 2nd ed. John Wiley; 2006.
[19] Ackermann T. Wind power in power systems. John Wiley; 2006.
[20] Pallabazzer R. Evaluation of wind-generator potentiality. Sol Energy 1995;55(1):49–59.
[21] Villanueva D, Pazos JL, Feijoo A. Probabilistic load flow including wind power generation. IEEE Trans Power Syst 2011;26(3):1659–67.
[22] Martins N, Henriques RM, Barbosa AA, Gomes S, Jr, Gomes CB, Martins ACB. Impact of induction motor loads in system loadability margins and damping of

tarjomehrooz.com 0902 795 28 76 ترجمه تخصصی توسط دکتری رشته مربوطه و برای کلیه زبان های خارجی + شبیه سازی مقالات با کلیه نرم افزار ها مثلب گمز و...

inter-area modes. In: Proc. of the IEEE PES General Meeting, vol. 2, 2003. p. 1379–84.
[23] Henriques R, Martins N, Ferraz JCR, Martins ACB, Pinto HJPC, Carneiro S, Jr. Impact of induction motor loads into voltage stability margins of large systems. In: Proc. of power systems computations conference, Seville, Spain, 2002.
[24] Burton T, Jenkins N, Sharpe D, Bossanyi E. Wind energy handbook. 2nd ed. John Wiley; 2011.
[25] Haque MH. Novel decoupled load flow method. IEE Proc C 1993;140(3):199–205.
[26] SimPowerSystems User's Guide, MathWorks, 2012.
[27] Haque MH, Rahim AHMA. Determination of first swing stability limit of a multimachine power systems. IEE Proc C 1989;136(6):373–9.
[28] Masters GM. Renewable and efficient electric power systems. Wiley Interscience; 2004.